OL | Organic Letters

Cite This: Org. Lett. XXXX, XXX, XXX−XXX

Letter

pubs.acs.org/OrgLett

Probing the Interconversion of Labdane Lactones from the Chinese Liverwort *Pallavicinia ambigua*

Yi Li,[†] Zejun Xu,[†] Rongxiu Zhu,[‡] Jinchuan Zhou,[§] Yan Zong,[†] Jiaozhen Zhang,[†] Mingzhu Zhu,[†] Xueyang Jin,[†] Yanan Qiao,[†] Hongbo Zheng,[†] and Hongxiang Lou*[,†]

[†]Department of Natural Products Chemistry, Key Lab of Chemical Biology (MOE), School of Pharmaceutical Sciences, Shandong University, Jinan 250012, China

[‡]School of Chemistry and Chemical Engineering, Shandong University, Jinan 250100, China

[§]School of Pharmacy, Linyi University, Linyi 276000, China

Supporting Information

ABSTRACT: We report on the spontaneous, reversible intramolecular transesterification of natural labdane lactones. Through extensive spectroscopic analysis, the interconversion between the two tautomers was investigated, which could be retarded when the free hydroxy group was acetylated or the exocyclic double bond of the lactone ring was mutated. Besides, a conversion mechanism was postulated, and the energy barriers were calculated by density functional theory calculations. Furthermore, the tautomers were found to inhibit the virulence of the efflux pump-deficient *Candida albicans* DSY654.

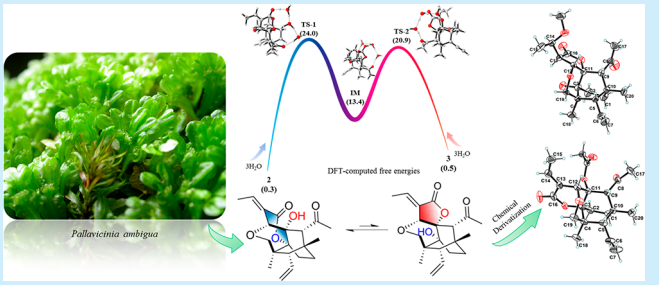

The abundant structural diversity of natural products has been driven by gene-encoded biosynthesis[1] combined with nonenzymatic modification[2] or isomerization,[3] which has led to the discovery of diverse bioactive compounds.[4] As a nonenzymatic isomerization method, interconversion plays an important role in the structural diversification of natural products (Figure 1), such as keto−enol tautomerism,[5] configurational equilibrium,[6] acetyl migration,[7] hydroxyaldehyde−hemiacetal interconversion or ring−chain tautomerism,[8] (retro-) oxa-Michael addition,[9] cis−trans isomerism,[10] atropisomerism,[11] as well as the photodriven interconversion of diterpenoids isolated from liverworts.[2,12]

Bryophytes are placed taxonomically between algae and pteridophytes.[13] Liverworts, as one of the three phyla of bryophytes, are rich in lipophilic terpenoids.[13b,14] Terpenoids constitute the most abundant and structurally diverse group of natural products,[15] of which labdane-type entities are widely distributed[16] and abundantly diversified via enzymatic or nonenzymatic pathways,[2,17] leading to various structurally different carbon skeletons. In recent years, a total of eight types of new labdane skeletons (pallavicinin, pallavicinolide,[18] pallambins A−D,[2,19] hapmnioides A−C,[3] and haplomintrins A−G[20]) have been found among more than 100 different labdane diterpenoids reported from liverworts,[21] which has led to several studies of their total synthesis due to their intriguing structures.[22]

Our ongoing investigation into the bioactive components from Chinese liverworts[20,23] has led to the discovery of five unprecedented labdane lactone pallamolides A−E (**1**−**5**) possessing a bicyclo[2.2.2]octane moiety and two new labdanes (**6** and **7**) from *Pallavicinia ambigua* (Mitt.) Stephani. (Figure 2) Among them, the tautomeric equilibriums of **2**/**3** and **4**/**5** were investigated and validated to be an intramolecular transesterification between the δ- and γ-lactone rings.

Pallamolide A (**1**) was isolated as a colorless crystal (in methanol) with the molecular formula $C_{20}H_{28}O_5$ determined by HRESIMS (*m*/*z* 366.2277 $[M + NH_4]^+$ (calcd 366.2275)). The ^{13}C NMR spectrum discovered two double bonds, an ester carbonyl and a ketone carbonyl, indicating that **1** was a three-ring structure in order to achieve its indices of hydrogen deficiency. Its ^1H NMR data (Table S1) showed four methyl signals at δ_H 0.79 (s), 1.23 (s), 2.01 (s), and 1.22 (t, J = 7.5 Hz), two protons of an oxygenated methylene at δ_H 3.89 (d, J = 11.5 Hz) and 3.47 (d, J = 11.5 Hz), and one terminal double bond at δ_H 5.18 (dd, J = 10.0, 2.0 Hz) and 4.96 (dd, J = 16.6, 1.5 Hz). The gross structure of **1** was constructed by a detailed analysis of the 1D and 2D NMR data (Figure 3). The linkage moieties $CH_2(1)-CH_2(2)$, $CH(5)-CH(6)-CH_2(7)$, and $CH_2(14)-CH_3(15)$ were established by the analysis of the $^1H-^1H$ COSY spectrum. The existence of an α-substituted γ-lactone ring was verified by the HMBC correlations from H-12 to C-11 (δ_C 89.3) and C-16 (δ_C 172.7) and from H-14 to C-12 and C-16. Moreover, the HMBC correlation from H-2 to C-3 and C-11, from H-5 to C-4, C-10, and C-9, and from H-9 to C-5, C-1, and C-11 implied the presence of a bicyclo[2.2.2]-

Received: November 28, 2019

Downloaded via SHANDONG UNIV on January 5, 2020 at 08:40:11 (UTC).
See https://pubs.acs.org/sharingguidelines for options on how to legitimately share published articles.

© XXXX American Chemical Society

DOI: 10.1021/acs.orglett.9b04270
Org. Lett. XXXX, XXX, XXX−XXX

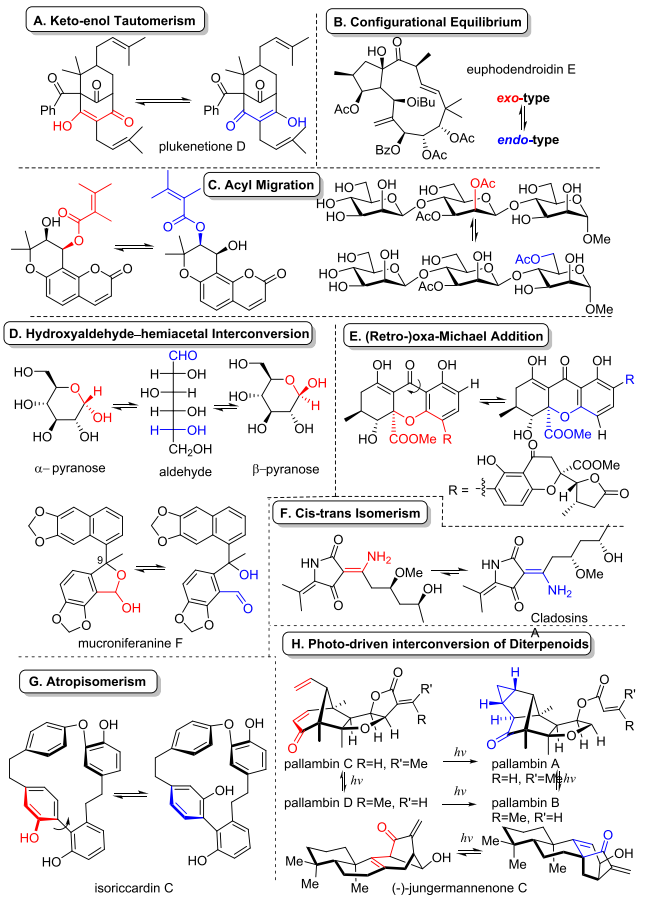

Figure 1. Examples of nonenzymatic interconversions of natural products.

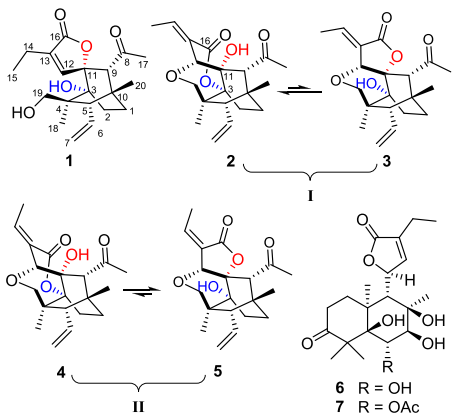

Figure 2. Structures of labdane lactones isolated from *P. ambigua*.

octane moiety. HMBC correlations of H_3-17/C-8 and H_3-18/C-19 suggested the assignment of the ketone carbonyl group and the oxygenated methylene, respectively. The aforementioned data indicated a 7,8-*seco*-labdane skeleton with a novel connection between C-3 and C-11 for **1**, as shown in Figure 2.

The NOESY correlations of H-5/H_3-20, H-5/H-9, and H_2-19/H-5 displayed the relative configuration of **1**. To determine the absolute configuration, single-crystal X-ray diffraction analysis with Cu Kα radiation was performed (CCDC 1947742, Figure 3). Consequently, the stereochemistry of **1** was proved to be 3R, 4S, 5S, 7S, 9R, 10R, 11R.

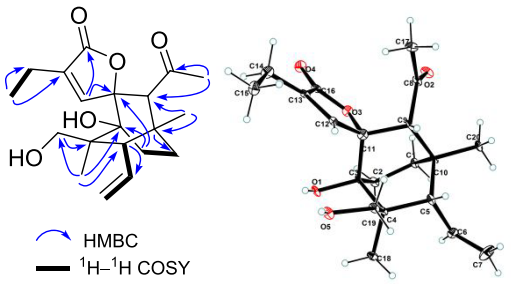

Figure 3. Selected HMBC (H → C),^{1}H–^{1}H COSY (H–H), and X-ray ORTEP drawing of **1**.

Additionally, two pairs of tautomers (**I** and **II**) containing similar carbon skeletons as **1** were obtained. Interconversion processes in deuterated solvents ($CD_3OD/CDCl_3$, Figure S1) and the 2D-TLC plate (Figure S2) were detected, and the tautomeric equilibriums were present in a ratio of approximately 3:2 and 1:2, respectively. Tautomer pairs **I** (pallamolides B (**2**) and C (**3**)) and **II** (pallamolides D (**4**) and E (**5**)) were identified to have the same molecular formula of $C_{20}H_{26}O_5$. In the 1D NMR, the signals of the major tautomer were inferred for **2**, whereas the remaining signals from **3** proved to be well differentiated. The observation of H-14 (δ_H 6.81 (qd, J = 7.3, 3.1 Hz)) and H-15 (δ_H 2.05 (dd, J = 7.3, 2.4 Hz)) indicated that the Δ^{12} in **1** was replaced by a Δ^{13} in **2**. Besides, the NMR data of C-12 (δ_C 82.5), together with the HMBC correlation between H-12 and C-19, suggested a six-membered oxygen ring in **2**, which coincides with the extra degree of unsaturation. The comprehensive analysis of the 2D NMR showed almost identical correlative patterns for **2** and **3**, although the 1D NMR data were obviously distinguishable from each other. Herein we hypothesized that the interconversion occurred because of an intramolecular transesterification, considering the structural characteristics of the ortho hydroxy groups at C-11 or C-3 for the formation of a 16,3-δ-lactone ring in **2** or a 16,11-γ-lactone ring in **3**, respectively. To confirm this hypothesis, we performed consecutive ^{13}C NMR experiments with equimolar amounts of tautomer **I** in CD_3OD and CD_3OH, respectively (Figure 4, Table S2). As expected, an α-isotope shift[24] of 0.1 ppm was measured at the exchangeable C-11 (**2**: major) or C-3 (**3**: minor) of tautomer **I**.

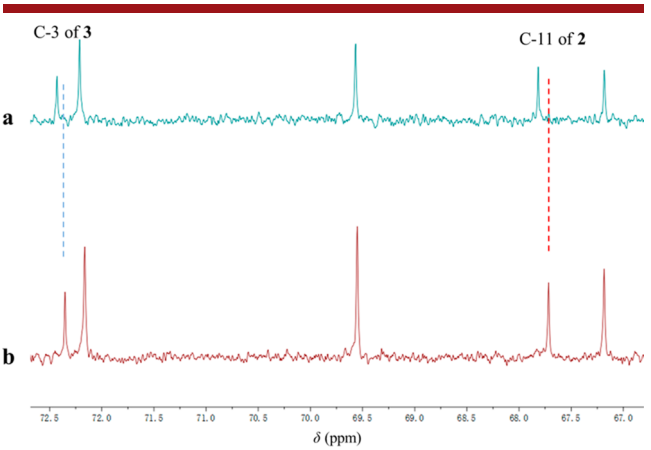

Figure 4. Partial ^{13}C NMR spectra of tautomer **I** in (a) CD_3OH and (b) CD_3OD at 150 MHz.

DOI: 10.1021/acs.orglett.9b04270
Org. Lett. XXXX, XXX, XXX–XXX

To retard this interconversion, we tried to methylate the free hydroxy, a key group that initiates the reaction. The methylation failed using CH_3I/Ag_2O, but an oxa-Michael addition product **3i** was obtained when using $MeOH/Et_3N$. (Figure 5a) The X-ray structure of **3i** (Figure 5b, CCDC

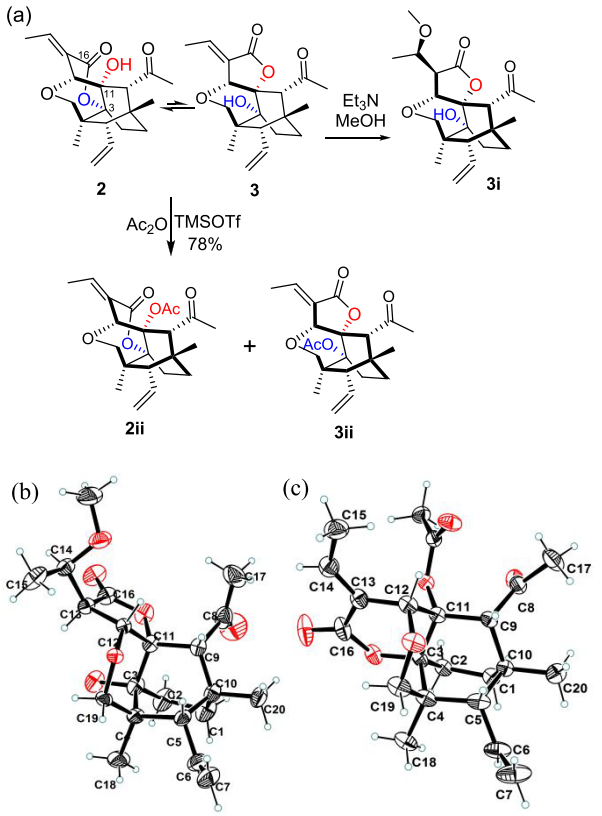

Figure 5. Chemical derivatization of tautomer **I** (a) and X-ray crystallographic structures of **3i** (b) and **2ii** (c).

1947415) confirmed the presence of a free 3-hydroxy in **2** and proved that this interconversion can be stopped by interfering with the exocyclic double bond. Furthermore, acetylation[25] with acetic anhydride gave two pure products, **2ii** and **3ii**, with C-11 and C-3 acetylated, respectively. The structure of **2ii** was determined by X-ray single-crystal diffraction analysis (Figure 5c, CCDC 1947743).

To gain better insight into the mechanism and probe the spontaneity of this intramolecular transesterification reaction, we performed quantum-chemical calculations of the transition states (TSs) and the reaction coordinate using density functional theory (DFT) at the PCM-B3LYP/6-31G* level. Considering that trace amounts of water exist in the solvents, the following cases were calculated for this interconversion reaction: the anhydrous reaction and the water-assisted reaction including concerted and stepwise mechanisms, with the assistance of one or two H_2O molecule(s) and $3H_2O$ cluster, respectively. In the cases of the anhydrous and one or two water-molecule-assisted reactions, all of the calculated energy barriers (Table S4) were too high to be spontaneously overcome for the interconversion reaction of tautomer **I** at room temperature. For the $3H_2O$-cluster-assisted interconversion, the two-step mechanism showed good agreement with the experimental phenomena. Figure S58 describes the potential energy surface (PES) for the tautomeric equilibrium. The reaction barrier from **2** to **3** is 24.5 kcal/mol, which is in accordance with the experimental conditions. Similarly, the inverse reaction from compound **3** to **2** also goes through the same pathway with a maximum energy barrier of 23.4 kcal/mol. Thus we speculated that during the interconversion between **2** and **3**, H_2O acted as a proton shuttle, making hydrogen atoms easier to transfer, which was confirmed by our experiment where we found that the interconversion rate between **2** and **3** was enhanced in the presence of water.

The typical differences of the chemical shifts at H_3-15, H-14, and H-12 between tautomers **I** and **II** proved that the configurations of the Δ^{13} were E and Z, respectively, considering the conjugation effect and magnetic anisotropy.[26] Besides, the NOESY correlations between H-12 and H-14 gave an accordant conclusion. The different ratios of **2**/**3** and **4**/**5** were probably caused by the Gibbs free-energy distinctions between the tautomers. Compounds **6** and **7** were also isolated as highly oxidized labdane lactones, of which congener **8** was a pivotal precursor in the proposed biosynthetic pathway (Scheme 1).

Scheme 1. Plausible Biosynthetic Pathway of 1−5

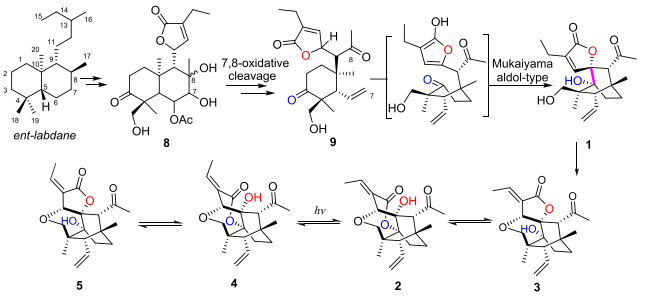

Because hyphae have been recognized as a crucial factor in biofilm formation and fungal virulence, we tested the effect of the isolated compounds (Table S5) against the *Candida albicans* morphological transition under various hyphae-inducing conditions in vitro by microphotography.[27] We found that tautomer **II** inhibited the hyphal formation of the efflux pump-deficient strain DSY654 in a dose-dependent manner in RPMI 1640 media, as illustrated in Figure 6A. In addition, the effect of tautomer **II** on the adhesion of *C. albicans* DSY654-*TDH3-GFP* to the surface of mammalian cells was further investigated. As shown in Figure 6B,C, tautomer **II** displayed an inhibition effect against the adhesion of DSY654-*TDH3-GFP* cells to A549 cells in a dose-dependent manner. Besides, *C. albicans* biofilm formation has been considered as a pivotal virulence factor because of its resistibility to antifungal agents and the capability against host immune defenses.[28] Accordingly, we explored whether the tautomers played a role in biofilm formation by using the XTT reduction assay. We observed that 16 μg/mL or more of tautomer **II** greatly destroyed the biofilm structure of DSY654 (Figure 6D,E). To clue the underlying mechanisms of the morphological transition and the cell adhesion inhibition effect induced by tautomer **II**, qPCR was performed to assess the transcriptional levels of hyphal growth and cell-adhesion-related genes in *C. albicans* when treated with tautomer **II**. We examined the mRNA levels of selected genes such as *Ras*1, *Dpp*3, *CDC*35, *EFG*1, *CEK*1, *NRG*1, *UME*6, *ALS*3, *HWP*1, and *ECE*1. As shown in Figure 6F, the transcriptional levels of three genes encoding adhesins, *ALS*3, *HWP*1, and *ECE*1, were significantly

DOI: 10.1021/acs.orglett.9b04270
Org. Lett. XXXX, XXX, XXX−XXX

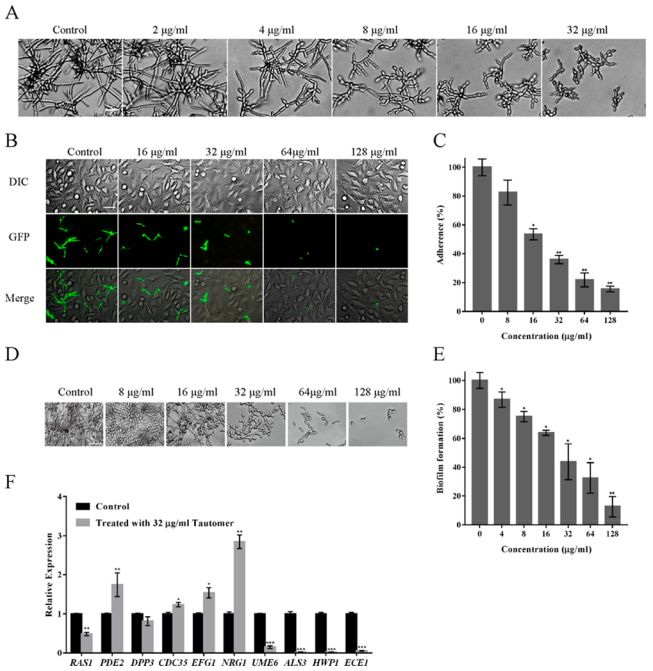

Figure 6. Inhibitory effects of tautomer **II** on *C. albicans* virulence factors. (A) Impact of tautomer **II** on hyphal formation. Filamentation was grown in RPMI 1640 medium with different concentrations at 37 °C. After 6 h of incubation, images were photographed using a microscope (scale bar: 25 μM). (B,C) Effect of tautomer **II** on the adhesion of *C. albicans*. A549 cells were coincubated with *C. albicans* DSY654-*TDH3*-*GFP* cells for 90 min. The fluorescent cells were observed using a fluorescence microscope (scale bar: 50 μM). The number was confirmed by counting the adherent cells in the pictures. Bars show the means ± SD. *P < 0.05, **P < 0.01, **P < 0.001. (D,E) Effect of tautomer **II** on the biofilm formation of *C. albicans*. Biofilms were grown in RPMI 1640 medium with different concentrations of tautomer **II** for 24 h. The biofilm was analyzed by the XTT reduction assay and visualized by a microscope (scale bar: 50 μM). *P < 0.05, **P < 0.01, **P < 0.001. (F) Expression of genes involved in hyphal formation and adhesion. *C. albicans* DSY654 was cultured in RPMI 1640 medium for 6 h under the treatment of tautomer **II** at 32 μg/mL. The transcriptional levels of genes were detected by qPCR. Bars represent the means ± SD. *P < 0.05, **P < 0.01, **P < 0.001.

decreased in the presence of tautomer **II**. Furthermore, the genes related to the Ras1-cAMP-Efg1 pathway (*Ras*1, *PDE*2, *Dpp*3, *CDC*35, *EFG*1, *NRG*1, and *UME*6) were downregulated to varying extents, whereas *PDE*2, which encodes a phosphodiesterase, was significantly upregulated after tautomer **II** treatment. Thus tautomer **II** inhibited the hyphal morphogenesis, adhesion, and biofilm formation of DSY654.

In this study, we investigated the tautomeric equilibrium of two pairs of novel skeleton labdanes, which was validated to be an intramolecular transesterification between the γ- and δ-lactone rings by extensive NMR spectroscopic studies, chemical derivatization, and DFT calculations. Interconversion of the tautomers was terminated by converting the exocyclic double bond into a single bond, as in **3i** or transferring it into the lactone ring, as in **1**, possibly due to the low ring-strain energy.[29] Meanwhile, blocking the *o*-hydroxy group of the lactone ring in the tautomers could also impede the tautomeric reaction. Our findings might also stimulate further consideration of the involvement of the intramolecular transesterification of drugs or lead compounds that possess exocyclic double bonds and *o*-hydroxy groups on a lactone ring as well as their application in synthetic chemistry.

■ ASSOCIATED CONTENT

Supporting Information

The Supporting Information is available free of charge at https://pubs.acs.org/doi/10.1021/acs.orglett.9b04270.

Structure elucidation of compounds **6** and **7**; general experimental procedures, thermodynamic parameters, and coordinates for the calculated structures; 1D and 2D NMR data; HRESIMS, IR, UV, and CD spectra of the new compounds; TLC and NMR analysis for the interconversion; details of the DFT calculations; and bioactivity of tautomer **II** (PDF)

Accession Codes

CCDC 1947415 and 1947742−1947743 contain the supplementary crystallographic data for this paper. These data can be obtained free of charge via www.ccdc.cam.ac.uk/data_request/cif, or by emailing data_request@ccdc.cam.ac.uk, or by contacting The Cambridge Crystallographic Data Centre, 12 Union Road, Cambridge CB2 1EZ, UK; fax: +44 1223 336033.

■ AUTHOR INFORMATION

Corresponding Author

*Email: louhongxiang@sdu.edu.cn.

ORCID

Hongxiang Lou: 0000-0003-3300-1811

Notes

The authors declare no competing financial interest.

■ ACKNOWLEDGMENTS

This work was financially supported by the National Natural Science Foundation of China (81874293 and 81630093). We acknowledge the Center of Pharmaceutical Analysis (Shandong University) for testing spectroscopic data. We are grateful to Prof. Jian Zhang (Shandong University) for the X-ray crystallography analysis.

■ REFERENCES

(1) (a) Podust, L. M.; Sherman, D. H. *Nat. Prod. Rep.* **2012**, *29*, 1251−1266. (b) Dixon, R. A. *Curr. Opin. Biotechnol.* **1999**, *10*, 192−197.

(2) Zhang, J.-Z.; Zhu, R. X.; Li, G.; Wang, L. N.; Sun, B.; Chen, W. F.; Liu, L.; Lou, H. X. *Org. Lett.* **2012**, *14*, 5624−5627.

(3) Zhou, J. C.; Zhang, J. Z.; Li, R. J.; Liu, J.; Fan, P. H.; Li, Y.; Ji, M.; Dong, Y. W.; Yuan, H. Q.; Lou, H. X. *Org. Lett.* **2016**, *18*, 4274−4276.

(4) (a) Morrison, K. *Ann. Trop. Paediatr.* **2013**, *12*, 55−66. (b) Magadula, J. J.; Erasto, P. *Nat. Prod. Rep.* **2009**, *26*, 1535−1554.

(5) (a) Henry, G. E; Jacobs, H.; McLean, S.; Reynolds, W. F; Yang, J.-P. *Tetrahedron Lett.* **1995**, *36*, 4575−4578. (b) Henry, G. E.; Jacobs, H.; Carrington, C. M. S.; Mclean, S.; Reynolds, W. F. *Tetrahedron* **1999**, *55*, 1581−1596.

(6) Esposito, M.; Nothias, L.-F.; Nedev, H.; Gallard, J. F.; Leyssen, P.; Retailleau, P.; Costa, J.; Roussi, F.; Iorga, B. I.; Paolini, J.; et al. *J. Nat. Prod.* **2016**, *79*, 2873−2882.

(7) (a) Yang, A. R.; Lee, S.; Yoo, Y. D.; Kim, H. S.; Jeong, E. J.; Rho, J.-R. *J. Nat. Prod.* **2017**, *80*, 1688−1692. (b) Deshpande, S.; Jaiswal, R.; Matei, M. F.; Kuhnert, N. *J. Agric. Food Chem.* **2014**, *62*, 9160−9170. (c) Lassfolk, R.; Rahkila, J.; Johansson, M. P.; Ekholm, F. S.; Wärnå, J.; Leino, R. *J. Am. Chem. Soc.* **2019**, *141*, 1646−1654.

DOI: 10.1021/acs.orglett.9b04270
Org. Lett. XXXX, XXX, XXX−XXX

(8) (a) Elix, J. A.; Ferguson, B. A.; Sargent, M. V. *Aust. J. Chem.* **1974**, *27*, 2403−2411. (b) Millot, M.; Tomasi, S.; Articus, K.; Rouaud, I.; Bernard, A.; Boustie, J. *J. Nat. Prod.* **2007**, *70*, 316−318. (c) Zhang, J.; Zhang, Q. Y.; Tu, P. F.; Xu, F. C.; Liang, H. *J. Nat. Prod.* **2018**, *81*, 364−370. (d) Lewis, B. E.; Choytun, N.; Schramm, V. L.; Bennet, A. J. *J. Am. Chem. Soc.* **2006**, *128*, 5049−5058.
(9) (a) Wu, G.; Yu, G.; Kurtán, T.; Mándi, A.; Peng, J.; Mo, X.; Liu, M.; Li, H.; Sun, X.; Li, J.; Zhu, T.; Gu, Q.; Li, D. *J. Nat. Prod.* **2015**, *78*, 2691−2698. (b) Mai, J.; Hoxha, E.; Morton, C. E.; Muller, B. M.; Adler, M. J. *Org. Biomol. Chem.* **2013**, *11*, 3421−3423. (c) Qin, T.; Iwata, T.; Ransom, T. T.; Beutler, J. A.; Porco, J. A. *J. Am. Chem. Soc.* **2015**, *137*, 15225−15233.
(10) Wu, G.; Sun, X.; Yu, G.; Wang, W.; Zhu, T.; Gu, Q.; Li, D. *J. Nat. Prod.* **2014**, *77*, 270−275.
(11) (a) Wang, L. N.; Xie, C. F.; Zhu, X. S.; Fan, P. H.; Lou, H. X. *J. Asian Nat. Prod. Res.* **2011**, *13*, 312−318. (b) Bringmann, G.; Muehlbacher, J.; Reichert, M.; Dreyer, M.; Kolz, J.; Speicher, A. *J. Am. Chem. Soc.* **2004**, *126*, 9283−9290. (c) Scher, J. M.; Zapp, J.; Becker, H.; Kather, N.; Kolz, J.; Speicher, A.; Dreyer, M.; Maksimenka, K.; Bringmann, G. *Tetrahedron* **2004**, *60*, 9877−9881.
(12) Hong, B.; Liu, W.; Wang, J.; Wu, J.; Kadonaga, Y.; Cai, P. J.; Lou, H. X.; Yu, Z. X.; Li, H.; Lei, X. *Chem.* **2019**, *5*, 1671−1681.
(13) (a) Asakawa, Y.; Ludwiczuk, A.; Nagashima, F. *Prog. Chem. Org. Nat. Prod.* **2013**, *95*, 563−605. (b) Asakawa, Y.; Ludwiczuk, A. *J. Nat. Prod.* **2018**, *81*, 641−660.
(14) Asakawa, Y. *Curr. Pharm. Des.* **2008**, *14*, 3067−3088.
(15) Kouloura, E.; Tchoumtchoua, J.; Halabalaki, M.; Skaltsounis, A. L. In *Encyclopedia of Analytical Chemistry*, 2014; pp 1−53.
(16) Hanson, J. R. *Nat. Prod. Rep.* **2015**, *32*, 76−87.
(17) Peters, R. J. *Nat. Prod. Rep.* **2010**, *27*, 1521−1530.
(18) (a) Chia-Li, W.; Huei-Ju, L.; Huey-Ling, U. *Phytochemistry* **1994**, *35*, 822−824. (b) Toyota, M.; Saito, T.; Asakawa, Y. *Chem. Pharm. Bull.* **1998**, *46*, 178−180.
(19) Wang, L. N.; Zhang, J. Z.; Li, X.; Wang, X. N.; Xie, C. F.; Zhou, J. C.; Lou, H. X. *Org. Lett.* **2012**, *14*, 1102−1105.
(20) Zhou, J. C.; Zhang, J. Z.; Cheng, A. X.; Xiong, Y. X.; Liu, L.; Lou, H. X. *Org. Lett.* **2015**, *17*, 3560−3563.
(21) Liu, N.; Wu, C.; Wang, P.; Lou, H. X. *Curr. Org. Chem.* **2018**, *22*, 1847−1860.
(22) (a) Ebner, C.; Carreira, E. M. *Angew. Chem., Int. Ed.* **2015**, *54*, 11227−11230. (b) Martinez, L. P.; Umemiya, S.; Wengryniuk, S. E.; Baran, P. S. *J. Am. Chem. Soc.* **2016**, *138*, 7536−7539. (c) Huang, B.; Guo, L.; Jia, Y. *Angew. Chem., Int. Ed.* **2015**, *54*, 13599−13603.
(23) (a) Zhang, C. Y.; Gao, Y.; Zhu, R. X.; Qiao, Y. N.; Zhou, J. C.; Zhang, J. Z.; Li, Y.; Li, S. W.; Fan, S. H.; Lou, H. X. *J. Nat. Prod.* **2019**, *82*, 1741−1751. (b) Han, J. J.; Zhang, J. Z.; Zhu, R. X.; Li, Y.; Qiao, Y. N.; Gao, Y.; Jin, X. Y.; Chen, W.; Zhou, J. C.; Lou, H. X. *Org. Lett.* **2018**, *20*, 6550−6553.
(24) Hansen, P. E. *Annu. Rep. NMR Spectrosc.* **1984**, *15*, 105−234.
(25) Procopiou, P. A.; Baugh, S. P. D.; Flack, S. S.; Inglis, G. G. A. *J. Org. Chem.* **1998**, *63*, 2342−2347.
(26) Bovey, F. A.; Jelinski, L.; Mirau, P. A. In *Nuclear Magnetic Resonance Spectroscopy*, 2nd ed.; Bovey, F. A., Jelinski, L., Mirau, P. A., Eds.; Academic Press: San Diego, 1988; pp 87−146.
(27) Sudbery, P.; Gow, N.; Berman, J. *Trends Microbiol.* **2004**, *12*, 317−324.
(28) Nett, J.; Andes, D. *Curr. Opin. Microbiol.* **2006**, *9*, 340−345.
(29) (a) Saiyasombat, W.; Molloy, R.; Nicholson, T. M.; Johnson, A. F.; Ward, I. M.; Poshyachinda, S. *Polymer* **1998**, *39*, 5581−5585. (b) Khoury, P. R.; Goddard, J. D.; Tam, W. *Tetrahedron* **2004**, *60*, 8103−8112. (c) Binda, P.; Barnes, Z.; Guthrie, D.; Ford, R. *Open J. Polym. Chem.* **2017**, *7*, 76−91.

DOI: 10.1021/acs.orglett.9b04270
Org. Lett. XXXX, XXX, XXX−XXX